Miniaturized bioactivity screening of complex samples

Heus, F.A.H.

2015

document version
Publisher's PDF, also known as Version of record

Chapter 6

High-Resolution Fractionation after Gas Chromatography for Effect-Directed Analysis

Eelco Pieke[1], Ferry Heus[1], Jorke H. Kamstra[2], Marija Mladic[1], Martin van Velzen[2], Dik Kamminga[1], Marja H. Lamoree[2], Timo Hamers[2], Pim Leonards[2], Wilfried M.A. Niessen[1,3] and Jeroen Kool[1]

(1) Division of BioMolecular Analysis, Department of Chemistry and Pharmaceutical Sciences, Faculty of Sciences, VU University Amsterdam, De Boelelaan 1083, 1081 HV Amsterdam, The Netherlands
(2) Institute for Environmental Studies (IVM), Faculty of Earth and Life Sciences, VU University Amsterdam, De Boelelaan 1085, 1081 HV Amsterdam, The Netherlands
(3) Hyphen MassSpec Consultancy, de Wetstraat 8, 2332 XT Leiden, The Netherlands

Analytical Chemistry, 2013. 85:8204

Abstract

This research presents an analytical technology for highly efficient, high-resolution, and high-yield fractionation of compounds after gas chromatography (GC) separations. The technology is straightforward, does not require sophisticated cold traps or adsorbent traps, and allows collecting large numbers of fractions during a GC run. The technology is based on direct infusion of a carrier solvent at the end of the GC column, where infusion takes place in the GC oven. Pentane and hexane used as carrier solvent showed good results. Acetonitrile also showed good results as a more polar carrier solvent. Development and optimization of the technology is described, followed by demonstration in a high-throughput effect directed analysis setting toward dioxin receptor bioactivity. The GC fractionation setup was capable of collecting fractions in the second range. As a result, fractionated compounds could be collected into one or two fractions when 6.5 s resolution fractionation was performed. Subsequently, mixtures containing polycyclic aromatic hydrocarbons, of which some are bioactive toward the dioxin receptor, were profiled with a mammalian gene reporter assay. After fractionation into 96-well plates, we used our new approach for direct cell seeding onto the fractions prior to assaying which allowed dioxin receptor bioactivity to be measured directly after fractionation. The current technology represents a great advance in effect directed analysis for environmental screening worldwide as it allows combining the preferred analytical separation technology for often non-polar environmental pollutants with environmentally relevant bioassays, in high resolution.

Introduction

Current state-of-the-art fractionation of compounds after gas chromatography (GC) mostly requires complicated setups and only allows automated collection of a very limited number of fractions, usually only six, utilizing complicated cryo-trapping or adsorbent collection vessels [1–8]. As a result, postcolumn fractionation after liquid chromatography (LC) is used more frequently, even if GC is superior to LC for the mixtures to be separated and fractionated. Fractionation in LC is straightforward. LC fractionation setups are widespread when off-line analysis is to be performed after separation, e.g., for off-line bioassays in effect-directed analysis (EDA). The principle of EDA is to sequentially reduce the complexity of environmental, food, and/or technical mixtures by multiple fractionations (usually with low resolution [that is in the minutes range]) guided by biological activity [9–11]. Commonly used EDA approaches in environmental settings are directed toward the dioxin and estrogen receptors [10–12]. The biological activity found using EDA is to be correlated to the compound identities, mostly established with mass spectrometry (MS), but possibly assisted by nuclear magnetic resonance (NMR) and other spectroscopic techniques [12–14]. As low-resolution fractionation often results in fractions that still contain many compounds, each bioactive fraction has to be fractionated further, and the next series of fractions is to be tested again in the bioassay. This iterative fractionation strategy often fails to identify the bioactive

compounds since the bioactive fractions remain too complex for chemical identification, or compounds degrade or adhere to sample vials during the process. High-resolution fractionation after LC as described by Giera et al. [15] and Kool et al. [16] provided an advancement as fractions collected are in the seconds rather than minutes range. This allows a direct reconstruction of high-resolution bioactivity chromatograms and provides improved correlation between bioactivity and mass (as obtained by parallel postcolumn MS analysis) [15, 16].

Many compound classes, relevant in EDA, such as polycyclic aromatic hydrocarbons (PAHs), pesticides, and mineral oils are preferably analyzed by GC. Moreover, certified GC methodologies have been established in this area. Given the current limitations in GC fractionation, we decided to develop an alternative strategy. In this paper, we describe the development, optimization, validation, and application of a new GC fractionation strategy. Via a Y-shaped connector, positioned at the end of the GC column but still in the GC oven [17], a carrier solvent is continuously infused and mixed with the carrier gas flow. The gas–liquid mixture with the eluting compounds is collected in vials or, via a robotic device, in a 96-well microtiter plate (MTP). The volatile carrier solvent evaporates and leaves the fractionated compounds behind. In this way, the number of fractions can be drastically increased over currently available technology; fractions with seconds-range resolution can be collected. The fractionation technology developed was demonstrated in an environmental setting. Endocrine-disrupting pollutants in mixtures were identified as bioactives toward the dioxin receptor by using a mammalian cellular gene reporter assay as readout. In order to eliminate additional handling steps and prevent compound dilution, cells were seeded and grown postfractionation, directly onto the collected fractions.

Experimental

Chemicals

Development and optimization of the new GC fractionation system was performed using an in-house prepared stock solution (M12) containing the 12 halogenated compounds dissolved in *n*-hexane at a 10^{-2} M concentration: fenchlorphos (FCP; 4.87 ppm), tralomethrin (TM; 10.1 ppm), *cis*-chlorfenvinphos and *trans*-chlorfenvinphos (CFVP-a and CFVP-b; 5.45 ppm), bromophos-methyl (B; 5.54 ppm), 2,2′-dibromobiphenyl (2,2-DBB; 4,73 ppm), 4,4′-dibromobiphenyl (4,4-DBB; 4.73 ppm), chlorpyrifos (CCP; 5.31 ppm), *cis*-permethrin and *trans*-permethrin (PM-a and PM-b; 5.93 ppm), γ-cyhalothrin and λ-cyhalothrin (CHT-a and CHT-b; 6.81 ppm). CFVP, PM, and CHT were mixtures of their respective isomers. The 12 halogenated compounds, *n*-hexane, and lindane, to be used as internal standard (IS), were purchased from Sigma-Aldrich (Zwijndrecht, The Netherlands) with the PESTANAL brand, except 2,2′-dibromobiphenyl (97% purity). Benzo[a]pyrene (BaP; 98% purity solid) was purchased from Acros Organics (Geel, Belgium). The polycyclic aromatic hydrocarbon (PAH) standard mixture consisted of acenaphthylene (1) (25 ppm; 0.164 μM), acenapthene (2) (25 ppm; 0.162 μM), fluorene (3) (25 ppm; 0.150 μM), phenanthrene (4) (25 ppm; 0.140

μM), anthracene (5) (25 ppm; 0.140 μM), fluoroanthene (6) (25 ppm; 0.124 μM), pyrene (7) (25 ppm; 0.122 μM), benz[a]anthracene (8) (25 ppm; 0.110 μM), chrysene (9) (25 ppm; 0.110 μM), benzo[b]fluoroanthene (10) (25 ppm; 0.099 μM), benzo[k]fluoroanthene (11) (25 ppm; 0.099 μM), benzo[e]pyrene (12) (25 ppm; 0.099 μM), benzo[a]pyrene (13, BaP) (25 ppm; 0.099 μM), indeno[1,2,3-cd]pyrene (14) (25 ppm; 0.086 μM), dibenz[a,h]anthracene (15) (25 ppm; 0.090 μM) and benzo[ghi]perylene (16) (25 ppm; 0.090 μM). The environmental sample was harbor sediment Certified Reference Material 535 (CRM-535) obtained from NIST (Gaithersburg, MD, U.S.A.).

Procedure and Instrumentation Used for Development and Optimization

Separation

Mixture M12 was separated using a system as illustrated in Figure 1. The GC part of the system consisted of a Hewlett-Packard (Agilent Technologies, Palo Alto, CA, U.S.A.) HP6890 series GC oven (1) and auto injector (3), controlled by HP GC ChemStation 7.0 software. The FID detector (2) was not used in our setup. The split/splitless injection port (4) was equipped with a 11-mm Agilent septum and a Restek Sky 4.0 mm I.D. single taper/gooseneck inlet liner (5) (4.0 mm × 6.5 mm × 78.5 mm; Interscience, Breda, The Netherlands). The capillary column (6) was a Varian FactorFour VF-5 ms column (5% phenyl/95% dimethylpolysiloxane; 30 m × 0.37 mm × 250 μm I.D). The column exit was connected to a Restek Siltek MXT Y-union (7).

The injection volume of M12 was 1 μL, and the GC injection temperature was 300 °C using splitless mode. The purging of the split vent was started 2.0 min after injection with 20 mL/min helium. The GC oven was programmed from 65 °C (hold time 2.0 min) to 300 °C (hold time 8.0 min) at 15 °C/min. Praxair 5.0 grade helium (Vlaardingen, The Netherlands) was used as carrier gas and was kept at a constant column flow rate of 2.5 mL/min during the entire run, resulting in a head pressure of 170 kPa at 65 °C.

Preparation for Fractionation

As shown in Figure 1, the carrier gas from the GC column (8) was continuously mixed with a flow of *n*-hexane (or another solvent), which served as carrier liquid (9), via a Y-union. The liquid is delivered by a Harvard Apparatus (Holliston, MA, U.S.A.) HA22I syringe pump (10) equipped with a Hamilton (Bonaduz, Switzerland) GASTIGHT 1005C-XP 5 mL syringe (11), which was coupled to the Y-union via a Valco (VICI, Schenkon, Switzerland) zero-dead-volume connector (12), 135 cm of a 1/16-in. PEEK tubing (250 μm I.D.) (13), a second Valco zero-dead-volume connector (14), and the carrier liquid transfer line (~45 cm Restek Siltek deactivated fused silica, 250 μm I.D.) (15). Connections were made by chemically inert (PEEK) fingertight fittings. The Y-union was located in the GC oven. The resulting stream of carrier fluid, carrier gas, and eluting compounds (16) was directed via the outlet capillary (117 cm Restek Siltek deactivated fused silica, 340 μm I.D.) (17) to the exterior of the oven.

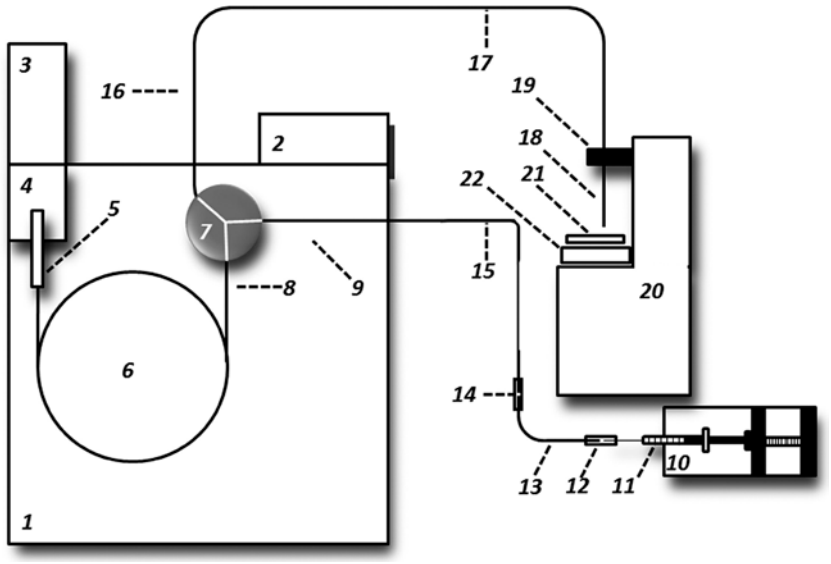

Figure 1. System setup of the GC fractionation system. Prior to the chromatographic separation, the GC oven (1) is programmed, and an optional standard (2) holding the cooling device is positioned. The sample is injected using an autoinjector (3) with splitless inlet (4). Through evaporation in the inert liner (5) the solvent plus analytes are transferred to the column (6), where they are separated and led through the Y-union (7) at the exit of the capillary column (8). In the Y-union, the carrier gas containing analytes is mixed with a carrier fluid entering from the liquid pump inlet (9). The fluid (11) is pumped through a carrier line (13–15) by a syringe pump (10). The carrier line consists of a zero-dead-volume connector piece (12) connected to PEEK tubing (13) which in turn is connected to a deactivated capillary (15) by another zero-dead-volume connector (14). The mixture of gas and fluid exits through the third opening of the Y-union, after which it can immediately be cooled using an optional stationary capillary cooler (16) held by a clamp (2). The direct or ambient cooled flow is then led to the X,Y,Z fractionation stage (20) via the outlet of the deactivated capillary (17). The arm of the X,Y,Z fractionation stage (19) moves the exit of the outlet capillary in a serpentine pattern over a well plate (21) held by an in-house-made well plate holder (22).

Fraction Collection and Recovery Analysis

Once outside of the GC oven, the outlet capillary was cooled by indirect heat exchange with the ambient air at room temperature (besides ambient air, also solid carbon dioxide (CO_2, −80 °C) and a solid CO_2/acetonitrile mixture (−40 °C) were tested using an in-house-built cooling trap). The exit of the outlet capillary (18) was connected to the XYZ arm (19) of a fractionator (20), holding a polystyrene 96-well MTP (Greiner Bio-One CELLSTAR, cat. no. 655180; Alphen a/d Rijn, The Netherlands) (21) in an in-house-built MTP holder (22). The fractionator was a modified Gilson (Den Haag, The Netherlands) 234 series auto injector, controlled by in-house-written software (‘GilsLua’; available upon request) and a Gilson 506C system interface. The fractions were collected in a serpentine pattern at a chosen fractionation resolution, programmed by the software.

Prior to recovery determination, the MTP was dried under a gentle stream of nitrogen. The fractions in the wells were redissolved in 200 μL of *n*-hexane; 50 μL of 10^{-8} M (4.40×10^{-6} ppm) lindane was added as IS. All fractions were analyzed by GC with electron-capture detection (GC-ECD). Detailed information can be found in the Supplementary material.

Postfractionation Bioassay Analysis

GC Fractionation

For fractionation, modifications to the GC program and settings were made. This information and relevant information on the parallel GC–MS analysis of the PAH standards and the CRM-535 sample can be found in the Supplementary material.

Bioassay Protocol and Analysis

Bioassay analysis was performed on Greiner polystyrene MTPs. First, the wells were coated by spotting 2.5 μL of 10% DMSO in water solution with a Thermo Scientific Multidrop Combi nL (Breda, The Netherlands), followed by evaporation of the water fraction under a nitrogen stream. This results in an end concentration of 0.25% DMSO after adding the cells. Fractions were collected onto the MTPs in a serpentine pattern, excluding the outer wells. Plates were dried under a nitrogen stream and stored at −20 °C until further use.

The potency to activate the dioxin or arylhydrocarbon receptor (AhR) was measured in the DR-LUC bioassay, consisting of the rat hepatoma cell line H4IIE, stably transfected with a luciferase construct under the transcriptional control of dioxin-responsive elements (DREs) [18]. Cell culturing and exposure was performed according to Murk et al. [19] with modifications. Cells were cultured in α-minimum essential medium (Gibco, Bleiswijk, The Netherlands) supplemented with 10% fetal bovine serum (Sigma-Aldrich) and penicillin/streptomycin (Gibco). Prior to exposure, cells were suspended in complete medium. The 96-well MTPs with collected GC fractions were directly filled with the cell suspension (100 μL per well). In this way, cells were seeded postfractionation and were directly exposed to the fractions while also attaching to the bottoms of the wells. After exposure for 48 h, cells were visually checked for cytotoxic effects. Then, cells were lysed and measured for luciferase activity expressed in relative light units (RLU), according to Murk et al. [19]. The activities found were plotted against retention times of the collected fractions to obtain reconstructed bioactivity chromatograms.

Results and Discussion

This study describes a new approach for fractionation of compounds after GC. Figure 1 shows a schematic diagram of the setup. The outlet capillary from the Y-union is led to a fractionator holding a 96-well MTP in which the fractions are collected with a predetermined fractionation resolution (s/well). For optimization, compound recovery and fractionation resolution was evaluated using a synthetic mixture (M12, 1 μL of 10^{-5} M) and subsequent analysis of fractions by GC-ECD. The parameters under study were carrier solvent type, carrier solvent flow rate, helium pressure/flow rate, outlet carrier capillary length and diameter, position of the Y-union in GC oven, and effects of outlet carrier capillary cooling. Some parameters were evaluated by mixing the solvent and collecting the complete GC separation into one vial.

The biological application involved environmental profiling for AhR activating compounds using the dioxin-responsive luciferase reporter gene (DR-LUC) bioassay, which is at present the best screening method for dioxins and dioxin-like compounds [20–22].

Parameter Optimization

Hexane, pentane, methanol, and acetonitrile were each tested as carrier solvent at a flow rate of 170.0 μL/min by collecting the GC separation into one vial). With methanol, an average compound recovery of 39 ± 2% was found, whereas hexane, pentane and acetonitrile gave recoveries of 80 ± 2%, 85 ± 3%, and 90 ± 2%, respectively. When using *n*-pentane (boiling point of 36 °C) instead of hexane (boiling point of 68 °C) for fractionation on MPTs, very rapid evaporation of *n*-pentane is followed by evaporation of fractionated early eluting compounds. Acetonitrile was shown to dissolve plasticizers in the MTPs used. Thus, hexane was chosen as carrier solvent.

To evaluate the drying time, 200 μL portions of M12 were deposited in various nonadjacent wells. The wells were then allowed to dry under nitrogen stream for different time intervals, ranging from evaporated to dryness (after ~2 min) to 60 min. GC-ECD showed an (expected) correlation between elution time and evaporation profile (see Figure S1 in the Supplementary material). The early eluting compounds largely decreased in recovery even after a few minutes of drying, whereas the later-eluting compounds showed little or no recovery loss, and only after complete evaporation of hexane.

Different carrier solvent flow rates (84, 170, 340, and 700 μL/min) were tested at a low resolution (30 s/well) to determine the optimum flow rate. High solvent flow rates caused a notable side effect: delay in compound elution due to backpressure effects. There appeared not to be a distinct optimum flow rate as recoveries were similar for the range tested (see Supplementary material Figure S2a). The last eluting compound, TM, showed a remarkably low recovery with a high deviation, which might be due to its poor solubility in hexane and its high boiling point (~594 °C). Similar broadening effects and low recovery, however, were observed for TM when using the more polar carrier solvent, acetonitrile.

In a subsequent high-resolution fractionation experiment (6.5 s/well), only the first five peaks were collected in order to reduce the number of fractions to be reanalyzed. The results (displayed in the Supplementary material Figure S2b) indicate similar recoveries for the compounds analyzed as for the 30 s/well fractions. At all carrier solvent flow rates tested, the GC peaks were collected into one or sometimes two fractions. A hexane solvent flow rate of 340 μL/min was chosen for further studies.

Fractionation of M12 was also performed at different helium carrier gas flow rates (1.0, 2.5 to 4.4 mL/min). Both high- and low-resolution fractionations were performed. The results showed that a recovery per compound of 80% or more is achieved in one analytical run for most compounds. The two higher flow rates gave slightly better recoveries. Performing a Student *t* test on the data revealed that a significant difference is observed between 2.5 mL/min and 4.4 mL/min. The highest flow rate tested (4.4 mL/min) showed a significant delay in compound elution due to the highest backpressure at the end of the GC column. Figure 2 shows the results obtained. At 6.5 s/well resolution, no effect at the resolution was observed. In only a few cases, a peak was distributed over more than one fraction. A flow rate of 2.5 mL was applied for further studies.

The length and inner diameter of the outlet carrier capillary and the position of the Y-union in the GC oven were shown not to have significant influence on recovery and resolution. Details can be found in the Supplementary material.

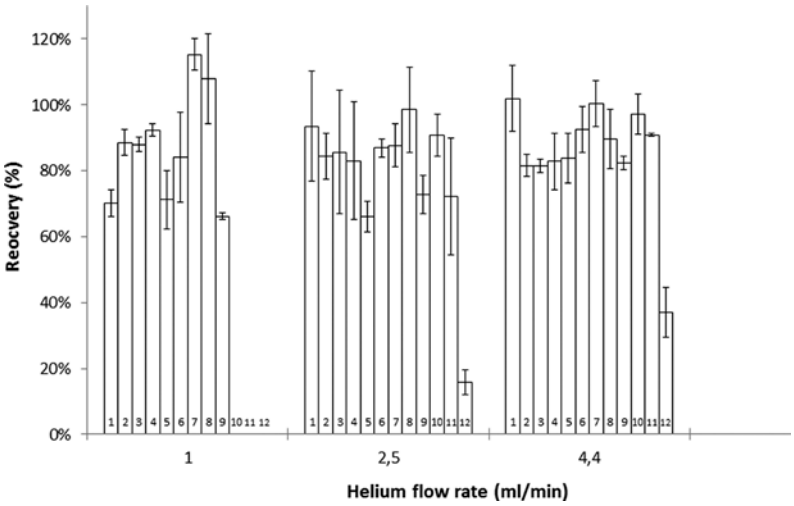

Figure 2. Relative recovery (in %) of the 12 compounds in the M12 mixture (see Supplementary material) as a function of the carrier gas flow rate (mL/min He at column exit).

Optional cooling of the outlet carrier capillary was achieved using an in-house-built cooling device by putting ~20 cm of the outlet carrier capillary in direct contact with coolant (solid carbon dioxide at −80 °C or a solid CO_2/acetonitrile mixture at −40 °C). Poor repeatability of the recovery was observed during tests at −80 °C between subsequent measurements. Some measurements with cooling at −80 °C gave good recoveries. Good recovery was obtained with −40 °C coolant (77 ± 14%), but an equally good recovery (76 ± 15%) was achieved by cooling at ambient air (20 °C).
In conclusion, the optimized conditions were 2.5 mL/min helium carrier gas, 340 μL/min hexane carried liquid flow, and 6.5 s/well fractionation into a white, nontransparent 96-well MTP.

Performance of the Analytical System after Optimization

After parameter optimization, the performance of the fractionation system was evaluated from recovery and resolution by fractionation of the M12 mixture under optimized conditions (6.5 s/well). The results are summarized in Figure 3. Good resolution is achieved for early eluting compounds like 2,2′-DBB, FCP, CCP and B, which are collected as one compound per well (Fig. 3A), whereas late eluting compounds like the coeluting isomers CHT-a and CHT-b, and PM-a and PM-b are distributed over a few wells (Fig. 3B). A 2D representation of Figure 3B including error bars is shown in the Supplementary material Figure S3. As the early eluting compounds are fractionated mostly in single fractions of 6.5 s, this demonstrates very limited post column band broadening of the system for these compounds. The recoveries observed in the high-resolution fractionation, however, are (systematically) lower than for fraction collection of a complete GC run into one container, or the 30 s resolution fractionation. This is most likely due to well to well movements that comprise relatively less time than in case of high 6.5 s resolution fractionation. Furthermore, evaporation effects of the low boiling compounds are stronger, because the high resolution leads to a much smaller volume of

carrier liquid per well. Fractionation with 3 s/well results in distribution of early eluting compounds over two wells (see Supplementary material Figure S4).

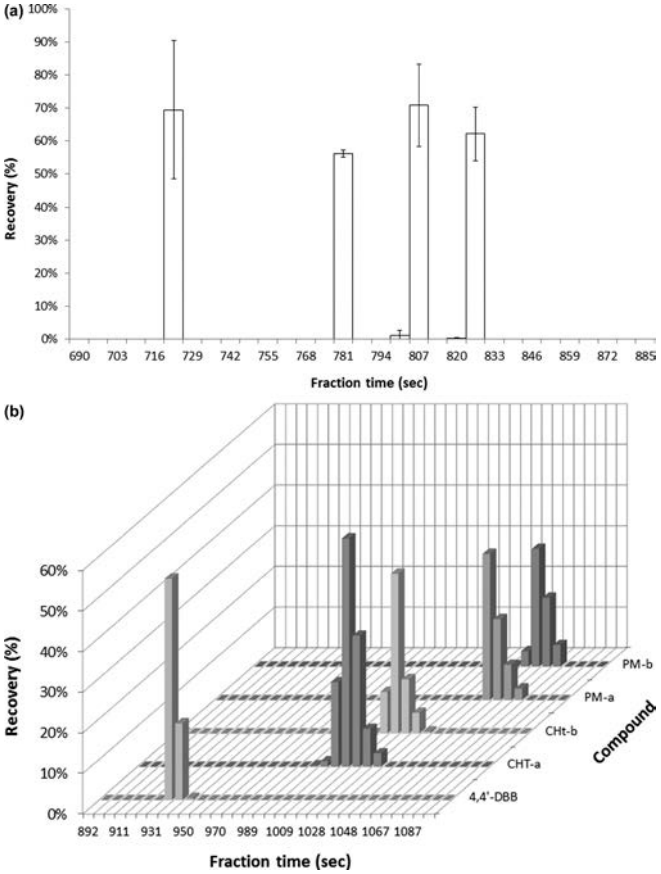

Figure 3. (A) Assessment of the fractionation resolution. 2,2′-DBB, FCP, CCP and B fractionated in high resolution with the optimized system in 6.5 s resolution. The compounds are listed in order of elution (the left-most compound being the first compound to elute from the column). The recovery in percentage is shown on the *y*-axis. The fraction time in seconds from injection is shown on the *x*-axis. (B) Five other peaks fractionated in high resolution with the optimized system in 6.5 s resolution. Due to coeluting compounds (most notably for the isomers) the figure has been plotted three-dimensionally. The peaks shown here are compounds that elute later than those shown in Figure 4A. As before, recovery is expressed as a percentage of the total on the *y*-axis, and the elution time in seconds is shown on the *x*-axis.

A shortcoming of GC using capillary columns is the low sample-loading amount. To address this shortcoming briefly, we performed repeated fractionation of the same sample on the same well plate, which demonstrated very repeatable fractionation of this sample over the same wells after repeated injections. In the Supplementary material, Figure S5 shows the results of the first five compounds in the M12 mixture fractionated 1, 3, and 5 times over the same wells. Figure S5 clearly shows that repeated fractionation of a sample over the same wells is possible, thus allowing up-concentration of the fractions by repeated fractionations.

DR-LUC Bioassay with PAH standards

An innovative way for cell seeding of adherent cells is applied in this study. In the postcolumn bioassay, the adherent cells are post-GC-fractionation seeded directly onto the dried fractions. In order to avoid nonspecific binding of the fractionated compounds to the wells, DMSO was deposited in the wells prior to fractionation. After evaporation of the carrier solvent, the often very nonpolar analytes reside in the thin DMSO film at the bottom of the wells, which facilitates dissolving during the assay.

As a first test, concentrations of 1000, 200, 40, and 8 ppm of BaP were injected and fractionated. After cell seeding, this would correspond to BaP concentrations in the bioassay well of 10 ppm [3.96×10^{-9} M], 2 ppm [7.92×10^{-10} M], 0.4 ppm [1.58×10^{-10} M] and 0.08 ppm BaP [3.17×10^{-11} M], if BaP would have been collected into one well. Actually, as is shown in Figure 4A, BaP was fractionated over multiple wells, thus lowering the actual concentrations in the wells. Fractionation time was plotted against RLU per fraction to generate reconstructed bioactivity chromatograms. Figure 4A shows four superimposed bioassay chromatograms from averaged duplicates of the four BaP concentrations analyzed. Bioactivity peaks were observed in the 550–600 s fractionation time range in a concentration response manner. The increased peak broadening at the higher BaP concentrations were found to be due to column overloading and not the result of fractionation. (This was independently demonstrated by GC-FID analysis; data not shown.) These results demonstrate the potential of direct post-GC column bioactivity screening without further chemical sample workup or pre-analysis steps.

Subsequently, a mixture containing 16 PAHs (5 ppm each) was analyzed. The resulting concentrations in the bioassay are at least a hundred fold lower than the injected concentrations since 1 μL is injected and the bioassay is performed in wells with 100 μL assay volume, i.e., medium and cells. Figure 4B shows the superimposed bioactivity chromatograms of a duplicate. In the bioactivity chromatograms obtained, several peaks can be clearly identified. The upper trace is the total-ion chromatogram (TIC) from GC–MS, obtained in parallel, from which the (partly coeluting) bioactive PAHs can be identified. An expanded view of the bioactive area between 11 and 18 min is shown in the Supplementary Material Figure S6. The bioactivity peak at 14.0 min corresponds to benz[a]anthracene (8) and/or chrysene (9). Machala et al. [23] showed that chrysene is more potent and is thus expected to give the largest contribution of the two. The rather broad bioactivity peak at 15.2 min was probably a combined bioactivity of benzo[b]fluoranthene (10), benzo[k]fluoranthene (11), benzo[e]pyrene (12) and benzo[a]pyrene (13). Murahashi et al. [22] showed that benzo[k]fluoranthene (11) is the strongest AhR binder of these PAHs, followed by benzo[b]fluoranthene (10). Note that Murahashi et al. [22] measured bioaffinity with a ligand binding assay rather than bioactivity in a cellular assay as we do. According to Machala et al., [23] the bioactivity at 15.2 min is largely caused by benzo[k]fluoranthene (11), as it is shown to be the most potent. The tailing of the peak at 15.2 min is caused by less bioactive compounds, such as benzo[a]pyrene (13). The bioactivity peak at 16.7 min consists of two coeluting compounds. Based on extracted ion chromatograms (EICs) (see Supplementary material Figure S7A), it was found that the double peak is due to overlapping indeno[1,2,3-cd]pyrene (14) and dibenz(a,h)anthracene (15), which are both known to be bioactive toward the AhR [22–27]. For all other PAHs analyzed, e.g., pyrene (7) and benzo[e]pyrene (12), no bioactivity was found with our approach, which is in agreement with data from Murahashi et al. [22] and Machala et al. [23].

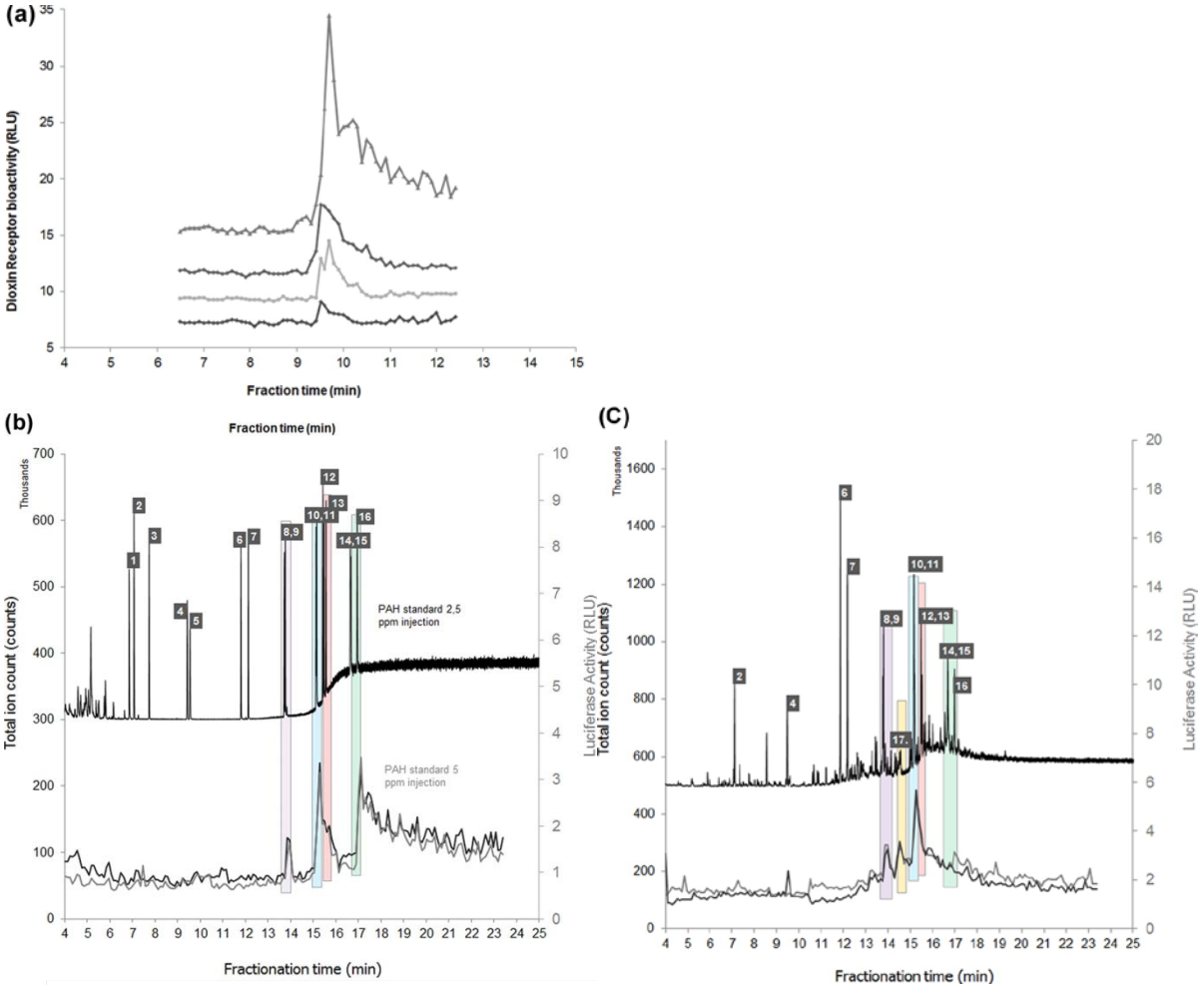

Figure 4. (A) GC fractionation with post column DR-bioassay. Four superimposed BaP chromatograms (averaged duplicates) are shown. Shown are the superimposed bioassay results from the GC-fractionation of a BaP standard injected in 10 ppm, 2 ppm, 0.4 ppm, and 0.08 ppm, respectively. The resulting relative light units (RLU) caused by the luciferase expressed from the gene reporter assay are plotted on the *y*-axis, while the fraction time in seconds is plotted on the *x*-axis. (B) Superimposed bioactivity chromatograms of a PAH mixture injected in duplicate in a 5 ppm concentration. Two clear bioactives are detected in a reproducible manner. Parallel GC–MS measurements (top chromatogram) allowed identification of the bioactives. The PAKs numbered 1 to 16 are described in the Experimental section. Coloured columns indicate correlation between bioactivity data and MS data. (C) Analysis of the CRM-535 sediment sample in duplicate. The lower superimposed chromatograms represent the bioassay chromatograms. The parallel obtained GC–MS data is represented as the top chromatogram. Bioactivity at peak 4 was observed but not reproducible.

DR-LUC Bioassay with CRM-535 Samples

Finally, an environmental sample containing PAHs (CRM-535) was analyzed. The data obtained are shown in Figure 4C. An expanded view of the bioactive area between 11 and 18 min is shown in the Supplementary material Figure S6. Comparison of the TIC shown in Figure 4Cwith that in Figure 4B shows that the PAH concentration in the CRM-535 sample was generally ~3–4 times lower. In the reconstructed bioactivity chromatograms, measured in duplicate, several bioactivity regions are found. Next to an intense bioactivity peak at 15.2 min, smaller peaks are visible near 14.0 and 14.5 min. Based on parallel GC–MS analysis, the same bioactive PAHs as observed for the standard mixture are observed for CRM-535, except for the three low-molecular-weight PAHs acenaphthylene (1), fluorene (3), and anthracene

(5). Thus, the peak at 14.0 min corresponds to benz[a]anthracene (8) and/or chrysene (9), the peak at 15.2 min to benzo[b]fluoranthene (10), benzo[k]fluoranthene (11), benzo[e]pyrene (12) and benzo[a]pyrene (13), with less bioactive compounds, such as benzo[a]pyrene (13), in the tail. CRM-535 showed no bioactivity peak at 16.7 min, but a peak was observed at 14.5 min. By background noise removal in the GC–MS data between 14.4 and 14.6 min (17 in Figure 4C), small peaks were identified. The MS library search identified these peaks as 12-methylbenz[a]anthracene, 1-methylchrysene and triphenylene. The bioactivity of these compounds for the dioxin receptor was confirmed by Cheung et al. [28]. The CRM sample showed no bioactivity at 16.7 min while the PAH standard did. The CRM-535 sample contained both compounds responsible for bioactivity in this area too, but in a lower indeno[1,2,3-cd]pyrene concentration and in a much lower dibenz[a,h]anthracene concentration, explaining the absence of a clear bioactive peak. EICs and the total ion count for both compounds in the PAH and the CRM-535 sample are shown in a and b of Figure S7 in the Supplementary material.

To test reproducibility, both the PAH standard and the CRM-535 sample were reanalyzed one month later. This yielded very similar results in terms of fractionation time shifts and recoveries (see Supplementary material Figure S8A and S8B).

Conclusions

We have developed, optimized and validated a postcolumn GC fractionation system enabling bioactivity assessment of 6.5 s fractions eluting from the GC column. The system allows fraction collection in 96-well MTP, thus enabling the collection of far more fractions than possible with commercial GC fractionation devices. Our technology shows robust behavior to a large range of variables tested and provides good recovery and resolution in fractionation. The GC fractionation setup was combined with a postcolumn DR-LUC bioassay to test bioactivity of individual compounds in a synthetic PAH mixture and in a commercial CRM-535 sample. In this, our postfractionation cell-seeding approach allowed for straightforward analysis without additional dilution and/or sample-handling steps for cellular assaying. Several bioactive PAHs were found in the PAH mixture and the CRM-535 sample, identified using parallel GC–MS analysis. This approach holds great promise for systematic application in EDA. One disadvantage of capillary GC is the low sample load, which can hamper postcolumn detection of bioactives when using bioassays less sensitive than the DR-LUC. This problem may be circumvented by using packed GC columns or, as demonstrated in this work by us, by fractionating multiple times in the same well plate.

Acknowledgments

F. Heus was financially supported with an ECHO Grant of the Dutch Scientific Society NOW (OND1221288 ECHO number 700.56.043). Stably transfected DR-LUC cells were kindly provided by Prof. Michael Denison (UC Davis, California, U.S.A.). Michiel Wijtten is thanked for the measurement of the repeated fractionations on one MTP. Jaap Schaap from Da Vinci is thanked for scientific advice and our ongoing collaboration towards valorization of the technology presented.

References

1. Ochiai, N.; Sasamoto, K., Selectable one-dimensional or two-dimensional gas chromatography-olfactometry/mass spectrometry with preparative fraction collection for analysis of ultra-trace amounts of odor compounds. J. Chromatogr., A 2011, 1218: 3180– 3185.
2. Meinert, C.; Moeder, M.; Brack, W., Fractionation of technical p-nonylphenol with preparative capillary gas chromatography. Chemosphere 2007, 70: 215– 223.
3. Mandalakis, M.; Gustafsson, Ö, Optimization of a preparative capillary gas chromatography-mass spectrometry system for the isolation and harvesting of individual polycyclic aromatic hydrocarbons. J. Chromatogr., A 2003, 996: 163– 172.
4. Yang, F. Q.; Wang, H. K.; Chen, H.; Chen, J. D.; Xia, Z. N., Fractionation of Volatile Constituents from *Curcuma* Rhizome by Preparative Gas Chromatography. J. Autom. Methods. Manag. Chem. 2011, 10.1155/2011/942467.
5. Meinert, C.; Brack, W., Optimisation of trapping parameters in preparative capillary gas chromatography for the application in effect-directed analysis. Chemosphere 2010, 78: 416– 422.
6. Meinert, C.; Schymanski, E.; Küster, E.; Kühne, R.; Schüürmann, G.; Brack, W.., Application of preparative capillary gas chromatography (pcGC), automated structure generation and mutagenicity prediction to improve effect-directed analysis of genotoxicants in a contaminated groundwater. Environ. Sci. Pollut. Res. Int. 2010, 17: 885– 897.
7. Holmstrand, H.; Mandalakis, M.; Zencak, Z.; Gustafsson, O.; Andersson, P., Chlorine isotope fractionation of a semi-volatile organochlorine compound during preparative megabore-column capillary gas chromatography. J. Chromatogr. A. 2006, 1103: 133– 138.
8. Özek, G.; Ishmuratova, M.; Tabanca, N.; Radwan, M. M.; Göger, F.; Özek, T.; Wedge, D. E.; Becnel, J. J.; Cutler, S. J.; Başer, K. H. C., One-step multiple component isolation from the oil of *Crinitaria tatarica* (Less.) Sojak by preparative capillary gas chromatography with characterization by spectroscopic and spectrometric techniques and evaluation of biological activity. J. Sep. Sci. 2012, 35: 650– 660.
9. Giesy, J. P.; Hilscherova, K.; Jones, P. D.; Kannan, K.; Machala, M., Cell bioassays for detection of aryl hydrocarbon (AhR) and estrogen receptor (ER) mediated activity in environmental samples. Mar. Pollut. Bull. 2002, 45: 3– 16.
10. Wölz, J.; Brack, W.; Moehlenkamp, C.; Claus, E.; Braunbeck, T.; Hollert, H., Effect-directed analysis of Ah receptor-mediated activities caused by PAHs in suspended particulate matter sampled in flood events. Sci. Total Environ. 2010, 408: 3327– 3333.
11. Iwasaki, S.; Kato, S.; Takahashi, M.; Kimura, T.; Sakka, K.; Ohmiya, K.; Matsuda, T.; Matsui, S., J. Biosci. Bioeng. 2004, 97: 216– 218.
12. Houtman, C. J.; Booij, P.; Jover, E.; Rio, D. P. d.; Swart, K.; Velzen, M. v.; Vreuls, R.; Legler, J.; Brouwer, A.; Lamoree, M. H., Analysis of estrogen-like compounds in the environment by high performance liquid chromatography bioassay. Chemosphere 2006, 65: 2244– 2252.
13. Schmitt, C.; Streck, G.; Lamoree, M.; Leonards, P.; Brack, W.; de Deckere, E., Effect directed analysis of riverine sediments--the usefulness of Potamopyrgus antipodarum for in vivo effect confirmation of endocrine disruption. Aquat. Toxicol. 2011, 101: 237– 243
14. Engwall, M.; Brunström, B.; Näf, C.; Hjelm, K., Levels of dioxin-like compounds in sewage sludge determined with a bioassay based on EROD induction in chicken embryo liver cultures. Chemosphere 1999, 38: 2327– 2343.
15. Giera, M.; Heus, F.; Janssen; Kool, J.; Lingeman, H.; Irth, H., Microfractionation revisited: a 1536 well high resolution screening assay. Anal. Chem. 2009, 81: 5460– 5466.
16. Kool, J.; de Kloe, G.; Denker, A. D.; van Altena, K.; Smoluch, M.; van Iperen, D.; Nahar, T. T.; Limburg, R. J.; Niessen, W. M.; Lingeman, H.; Leurs, R.; de Esch, I. J.; Smit, A. B.; Irth, H., Nanofractionation

spotter technology for rapid contactless and high-resolution deposition of LC eluent for further off-line analysis. Anal. Chem. 2011, 83: 125– 132.
17. Kool, J and Heus, F., Process to Separate Compounds Starting from a Mixture of Compounds. N2009010; Amsterdam Institute for Molecules, Medicines and Systems (AIMMS): Amsterdam, the Netherlands, 2012.
18. Garrison, P. M.; Tullis, K.; Aarts, J. M. M. J. G.; Brouwer, A.; Giesy, J. P.; Denison, M. S., Species-specific recombinant cell lines as bioassay systems for the detection of 2,3,7,8-tetrachlorodibenzo-p-dioxin-like chemicals. Appl. Toxicol. 1996, 30, 194– 203.
19. Murk, A. J.; Legler, J.; Denison, M. S.; Giesy, J. P.; Van de Guchte, C.; Brouwer, A., Chemical-activated luciferase gene expression (CALUX): a novel in vitro bioassay for Ah receptor active compounds in sediments and pore water. Fundam. Appl. Toxicol. 1996, 33, 149– 160.
20. He, G.; Tsutsumi, T.; Zhao, B.; Baston, D. S.; Zhao, J.; Heath-Pagliuso, S.; Denison, M. S., Third-generation Ah receptor-responsive luciferase reporter plasmids: amplification of dioxin-responsive elements dramatically increases CALUX bioassay sensitivity and responsiveness. Toxicol. Sci. 2011, 123: 511– 522.
21. Windal, I.; Denison, M. S.; Birnbaum, L. S.; Wouwe, N. V.; Baeyens, W.; Goeyens, L., Chemically activated luciferase gene expression (CALUX) cell bioassay analysis for the estimation of dioxin-like activity: critical parameters of the CALUX procedure that impact assay results. Environ. Sci. Technol. 2005, 39: 7357– 7364.
22. Murahashi, T.; Watanabe, T.; Kanayama, M.; Kubo, T.; Hirayama, T., Human Aryl Hydrocarbon Receptor Ligand Activity of 31 Non-substituted Polycyclic Aromatic Hydrocarbons as Soil Contaminants. J. Health. Sci. 2007, 53: 715– 721.
23. Machala, M.; Vondrácek, J.; Bláha, L.; Ciganek, M.; Neca, J. V., Aryl hydrocarbon receptor-mediated activity of mutagenic polycyclic aromatic hydrocarbons determined using in vitro reporter gene assay. Mutat. Res. 2001, 497: 49– 62.
24. Wenger, D.; Gerecke, A. C.; Heeb, N. V.; Zennegg, M.; Kohler, M.; Naegeli, H.; Zenobi, R., Secondary effects of catalytic diesel particulate filters: reduced aryl hydrocarbon receptor-mediated activity of the exhaust. Environ. Sci. Technol. 2008, 42: 2992– 2998.
25. Mason, G.G., Dioxin-receptor ligands in urban air and vehicle exhaust. Environ. Health. Perspect. 1994, 102 (Suppl 4): 111.
26. Soontjens, C. D.; Holmberg, K.; Westerholm, R. N.; Rafter, J., Characterization of polycyclic aromatic compounds in diesel exhaust particulate extract responsible for aryl hydrocarbon receptor activity. J. Atmos. Environ. 1997, 31: 219– 225.
27. Bittner, M.; Macikova, P.; Giesy, J. P.; Hilscherova, K., Enhancement of AhR-mediated activity of selected pollutants and their mixtures after interaction with dissolved organic matter. Environ. Int. 2011, 37: 960– 964.
28. Cheung, Y. L.; Gray, T. J. B.; Ioannides, C., Mutagenicity of chrysene, its methyl and benzo derivatives, and their interactions with cytochromes P-450 and the Ah-receptor; relevance to their carcinogenic potency. Toxicology 1993, 81: 69– 86.

Supplementary material

GC ECD analysis for recovery determination of collected fractions.

Preparation for recovery determination of collected fractions
In order to determine the recovery of the fractionated analytes of mixture M12, the entire well plate was dried by a gentle stream of nitrogen until near dryness. Then, each well was filled with 200 DL nAhexane, allowed to equilibrate for 30 sec and was then reAsuspended seven times with a GC syringe (Hamilton GASTIGHT 250 DL, Model 1725 Cemented NDL). Next, the content of each well was transferred to Aluglas 1.5 ml Amber, Wide Opening GC vials (32 × 11.6 mm) containing an insert (Aluglas 0.1 ml MicroAinsert, 29 × 5.7 mm with plastic spring). To this solution, 50 Dl of 10 A8M standard (lindane) was added. The resulting solution was then resuspended 5 times before capping the vials with Aluglas UltraClean Closure: 9mm polypropylene head, Silicone/PTFE septum caps for analysis. All fractions were subsequently analyzed by Gas Chromatography Electron Capture Detector (GCAECD) for recovery analysis. The peak areas of the analytes measured were corrected by using the standard (lindane).

Instrumental
The GC ECD system consisted of a Hewlett Packard (HP) 6890 series, a HP MicroAcell Electron Capture Detector (HAECD) and a Hewlett Packard 6890 series auto injector controlled by HP GC ChemStation software. The injection port type was split/splitless and the port was equipped with a 11 mm Agilent septum and lined with a Restek Sky 4.0mm ID Single Taper/Gooseneck Inlet Liner (4.0 x 6.5 x 78.5 mm). The column used was a FactorFour™ VFA5ms (5% phenyl/95%dimethylpolysiloxane) 30m x 0.37 mm x 0.25 Hm I.D. capillary column.

System parameters
The injection volume as 1 Dl with the injection port set at 300°C in splitless mode. To fully inject the sample, purge to split vent was started 2.0 min after injection with 20 mL/min helium. The GC oven was programmed from 65°C (hold time 2.00 min) to 300°C (hold time 2.00 min) at 15°C/min. Praxair 5.0 grade helium (Vlaardingen, The Netherlands) was used as carrier gas and was run in constant column flow mode. When using a flow rate of 4.4 mL/min, this resulted in a column head pressure of 250 kPa at 65°C. The ECD was run under constant makeup flow mode with Praxair 5.0 nitrogen (Vlaardingen, The Netherlands) at 30 mL/min. Detector sampling rate was set to 50 Hz at a temperature of 310°C. Chromatograms were manually integrated using HP ChemStation version 7.0.

Post fractionation bioassay analysis

GC fractionation
For BaP fractionation, modifications to the GC program and system were done: 100°C (hold time 1.00 min) to 300°C (hold time 8.00 min) at 40°C/min. Now, an ATAS OPTIC II injector was used to allow for large volume injections or programmed temperature injections. The ATAS injector, which was not controlled by HP ChemStation, was pressure programmed from 170 kPa (hold 1 min) to 270 kPa (hold 8 min) at 20 kPa/min. The pressure programming was performed since the OPTIC II does not support continuous flowmode and is not connected to the HP GC oven. The ATAS Optic II inlet pressure was programmed to maintain a constant flow at different oven temperatures, in order to match the program calculated by the HP ChemStation software. This calculation was performed by running a blank on the

unmodified 6890 series GC and storing the inlet pressure profile. For PAH fractionation, the OPTIC II injector was also used. The oven temperature program was adjusted to achieve baseline separation for most compounds. After injection, the oven was held at 80°C for 2 min, then at 30°C/min to 150°C and further at 15°C to 190°C, at which it was held for 2 min, then the temperature was raised to 270°C at 25°C/min and subsequently to 285°C at 10°C/min. Finally the temperature was raised to 320°C at 30°C/min, at which it was held (3 min) until the end of the run (17.87 min). Because the OPTIC II software does not support more than four pressure program points, the profile was simplified to best match the continuous flow program calculated by HP ChemStation. For this, the pressure was set at 177.0 kPa and held for 120 sec followed by raising to 240 kPa in 330s, raising to 312 kPa in 442s and finally held at 312 kPa for 181s.

GC–MS analysis of PAH standards and the CRM samples
For PAH and CRM analysis on GCAMS, identical methods were used to allow correlation between peaks. The injection was performed using an autoinjector with a 300°C injection port temperature in splitless mode. The PAH standard was diluted ten times and then injected, resulting in a 2.5 ppm injection. Purge to vent was set at 2.0 min with 50 mL/min Helium and column flow at 2.5 mL/min Helium. Temperature programming for oven was initially at 80°C (hold 2 min) and with 30°C/min to 150°C followed by 15°C/min to 190°C (hold 2 min). The hold was followed by 25°C/min ramp to 270°C, 10°C/min to 285°C and 30°C/min to 320°C at which the temperature was held for 10 min. The oven was then cooled to 50°C/min. Quadrupole MS detection parameters were 200°C for quadrupole and 250°C for source. EM volts was set at 1635 with a solvent delay at 3.0 min. Full scan mode was utilized between m/z = 50 and m/z = 300.

Outlet capillary length and diameter
Effects of the length of the outlet carrier capillary were assessed by cutting the respective capillary in half, resulting in a capillary of 54 cm, and reconnecting it. Afterwards, a 6.5s fractionation was performed with M12 collecting only the first 50 fractions for recovery and resolution tests. Results showed no significant change in recovery and resolution. Recovery averaged from two measurements was 83% ± 1%. All compounds were collected in the same fraction numbers as measurements with 117 cm of outlet. Next, the carrier capillary was removed and replaced by an equal length (117 cm) capillary with a larger ID of 320 Dm instead of 250 Dm. With this setup, a 6.5s fractionation was performed using M12 and collecting the first 50 fractions. Similar results were obtained: the average recovery for two fractionations was 88% ± 3%, with approximately the same elution times.

Depth of YAsplit in GC oven
In all previous experiments, the YAsplit was placed as high as possible in the GC oven, effectively placing it 1 cm near oven ceiling (and exit for the outlet capillary). In the current experiment, the YAsplit was lowered in the GC oven to 20 cm beneath the oven ceiling. Since in the current case, both the hexane flows (in and out) had a longer contact time in the oven, differences due to evaporation speed of hexane might occur. When the YAsplit was lowered in the GC oven, the average recovery was 85% ± 11% as compared to 83% ± 2% for measurement at 1 cm depth. There was however a notable difference between 1cm and 20cm measurements when looking at retention time shifts. The chromatograms and recovery/peak profiles were near equal, although there appeared to be a delay of ~13 more seconds in all collected fractions for the 20 cm depth measurements. The resolutions remained about the same effectively collecting all eluting compounds mostly in one or two fractions.

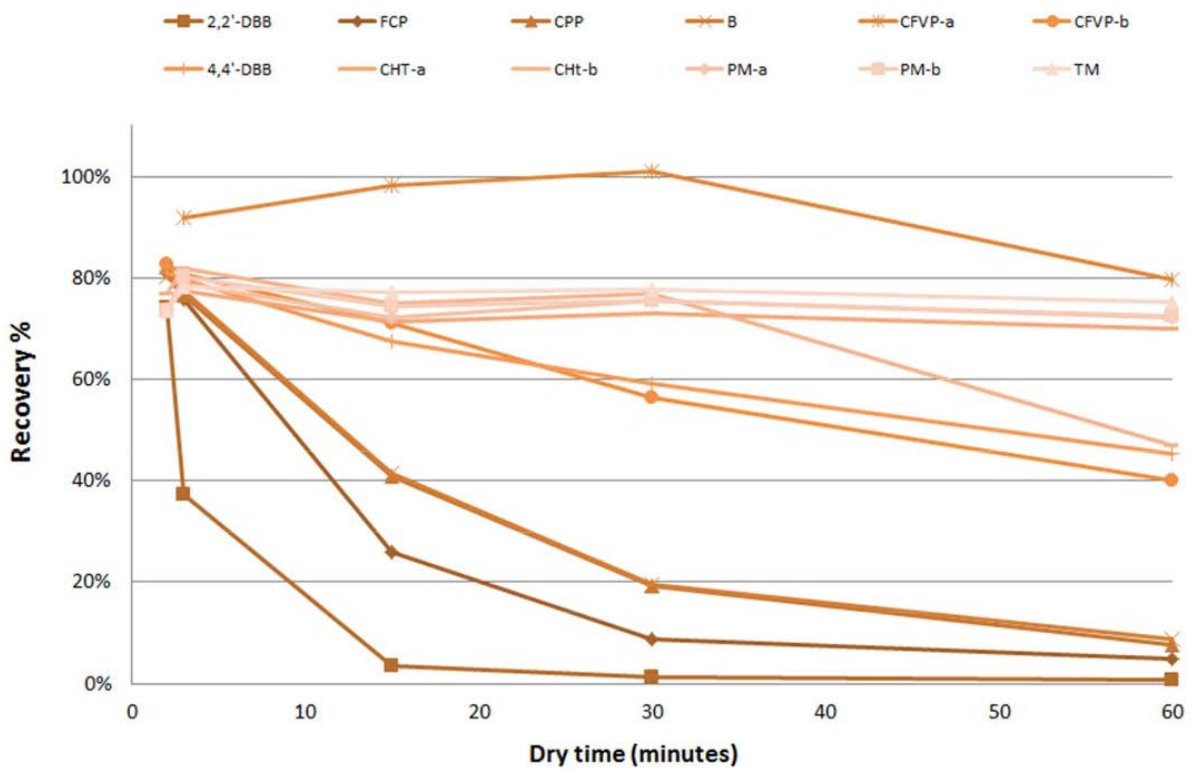

Figure S1. Correlation between dry time under a N^2 stream against the recovery of each compound fractionated. The x-axis is shown as drying time in minutes and the y-axis is shown as percent recovery after drying times. A darker colour indicates a lower boiling point compound. For the most volatile compounds, drying time significantly influences recovery after the fractionation step. For the less volatile compounds, there is a small influence. The highest boiling compounds are unaffected by drying time. The optimal drying time for solvent evaporation was to be as short as possible to prevent loss of volatile compounds.

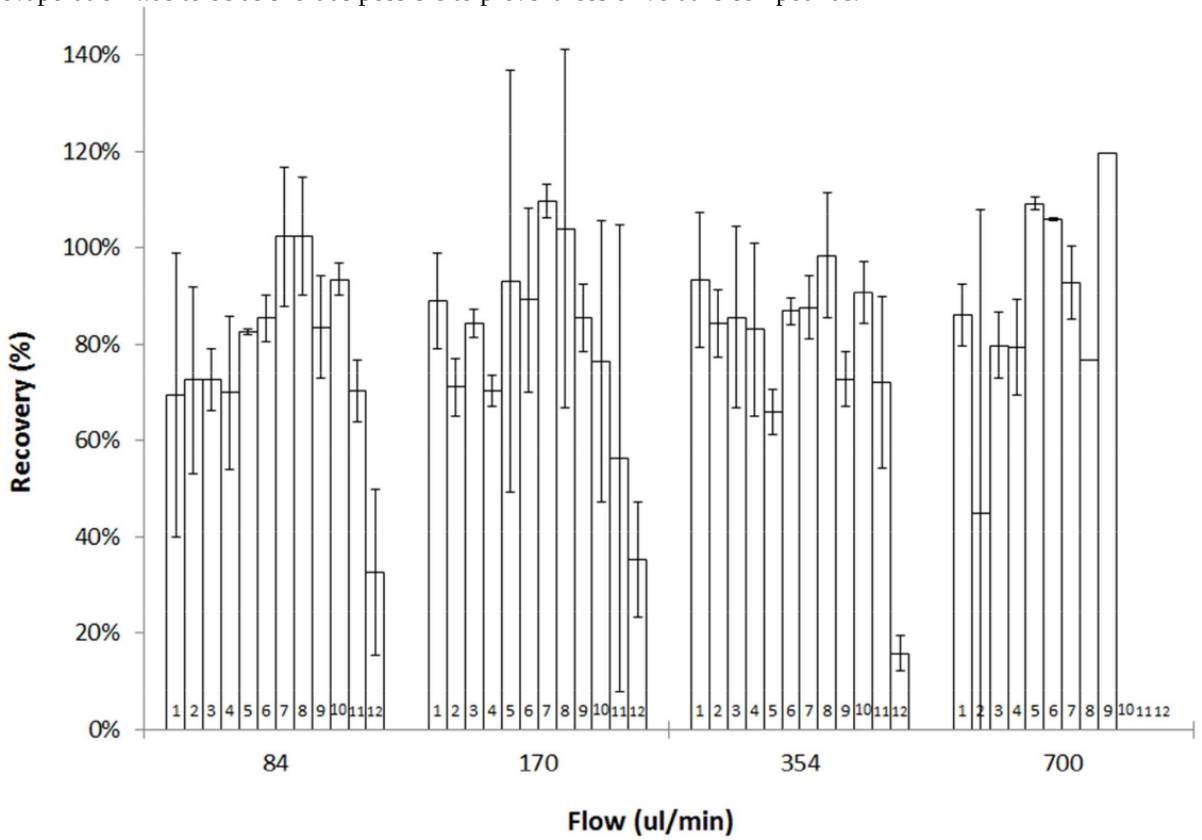

Figure S2A. Recovery per compound of mixture M12 at varying carrier fluid flow rates. The carrier fluid flow

rate is defined as the amount of carrier fluid exiting the outlet capillary during one minute (microliter/min) and is shown on the x-axis. The y-axis shows the relative recovery (%) per compound. Figure 2A lists the compounds in order of elution (the most upper compound being the first compound to elute from the column).The results show that a recovery per compound of 80% or more is achieved in one analytical run for most compounds.

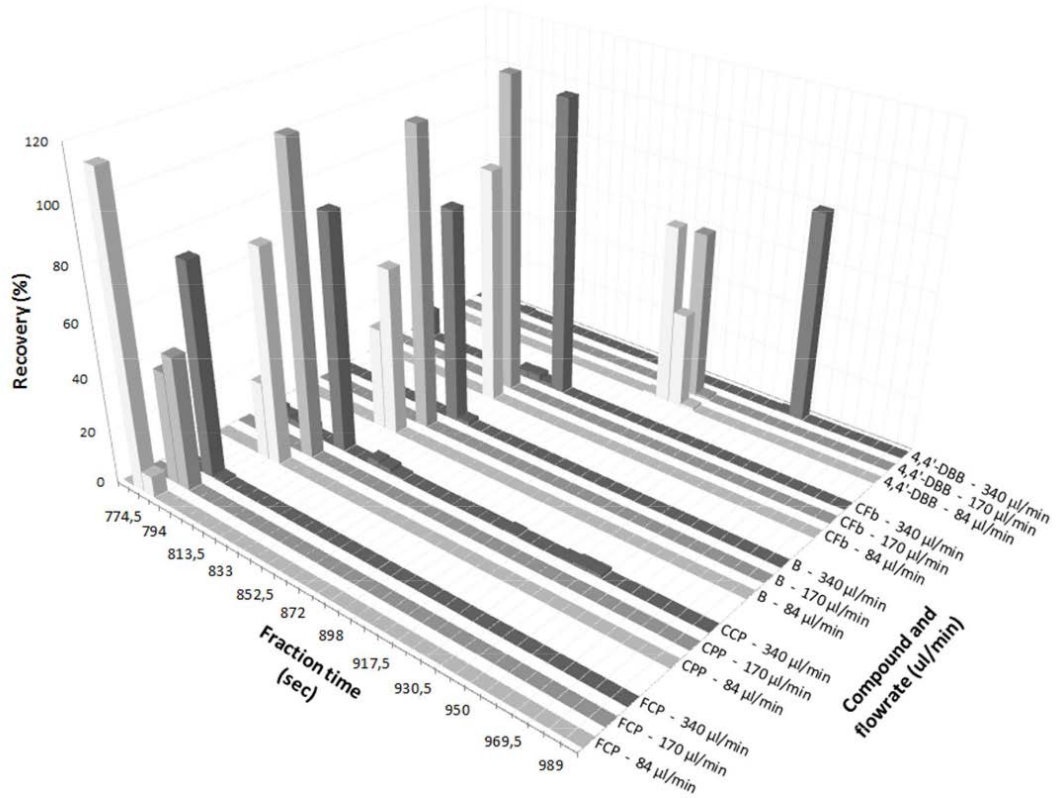

Figure S2B. Variation of the flow rate of the carrier solvent in high resolution demonstrated for five compounds. In this graph, different flow rates were tested at high resolution (6.5 sec/well) fractionation. The resulting recovery per fraction is on the y-axis. The fraction time from injection is shown on the x-axis. As can be seen, higher flow rates cause a larger retention time caused by backpressure on the exit of the GC column from the carrier solvent pump. Thus, although the fluid is able to pass through the capillary quicker, it is slowed by the build-up of pressure in the split. Recovery wise there is no significant difference between lower and higher flow rates. At higher flow rates there are fewer fractions per peak, reflecting slightly sharper peaks. Recoveries and standard deviations are depicted in Table S1.

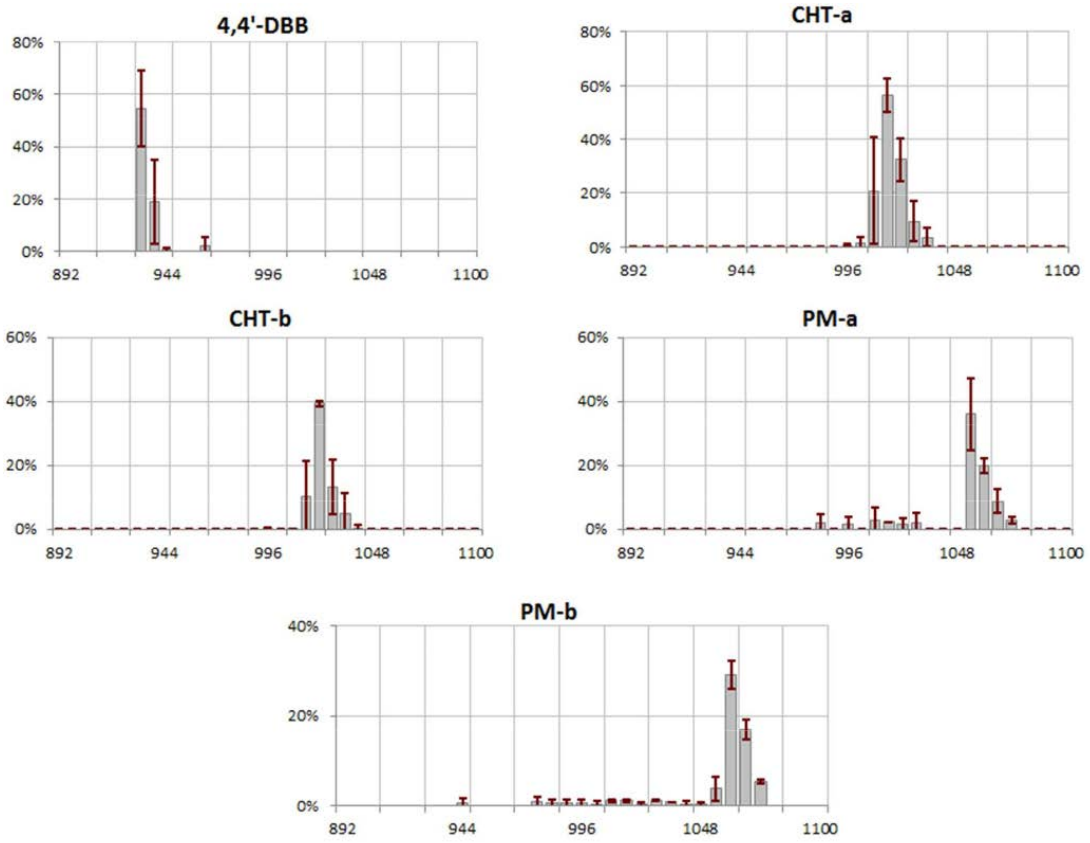

Figure S3. 2AD plots of five peaks fractionated in high resolution with the optimized system in 6.5 sec resolution. Standard deviations per fractions are shown as red bars. The x-axis is defined as the fraction time, while the y-axis is the recovery percentage per fraction. The sum of recoveries for all the fractions is the total recovery.

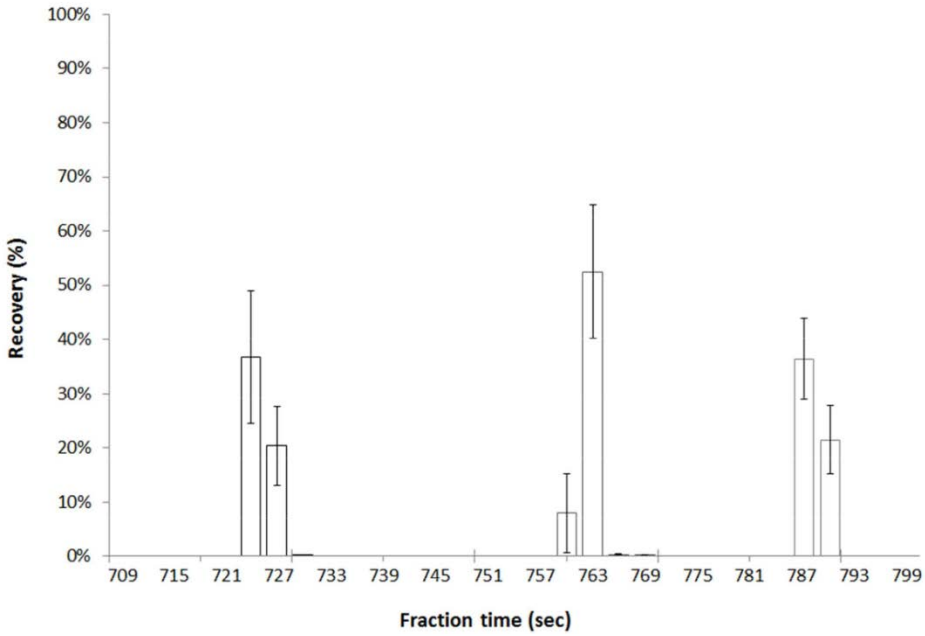

Figure S4. First three peaks eluted from mixture M12 fractionated in 3.0 sec high resolution. In this figure, the resolution is more than double the resolution used in Figures 4A and 4B. The peaks shown correspond to the first three peaks in Figure 4A. Again, recovery in percentage is plotted on the y-axis while elution time is shown on the x-axis in seconds. Peaks are now fractionated in two fractions. Recoveries are lower than for 6.5 sec/well fractionation because of evaporation effects and well to well movement effects.

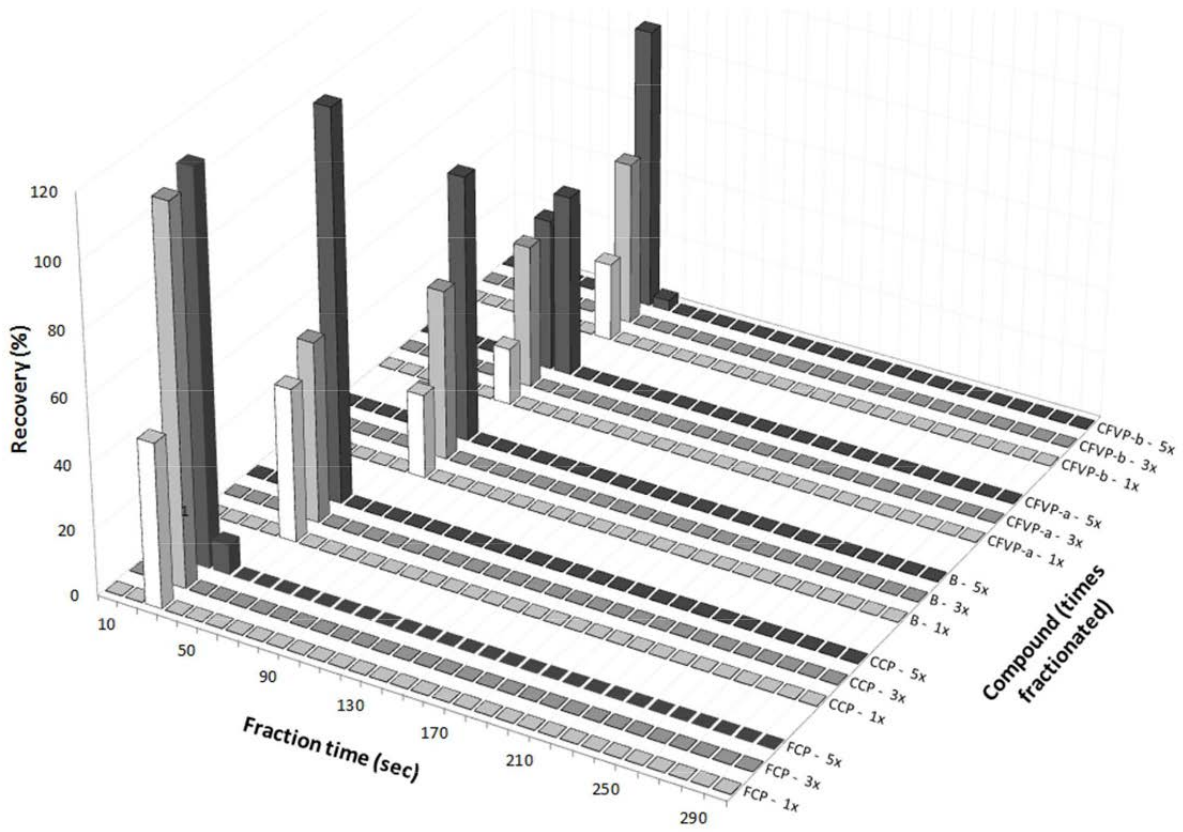

Figure S5. Shown are the results of the recovery of the first five compounds of the M12 mixture repeatedly fractionated over the same wells. per well per compound. Results of 1, 3 and 5 times repeated fractionations are shown.

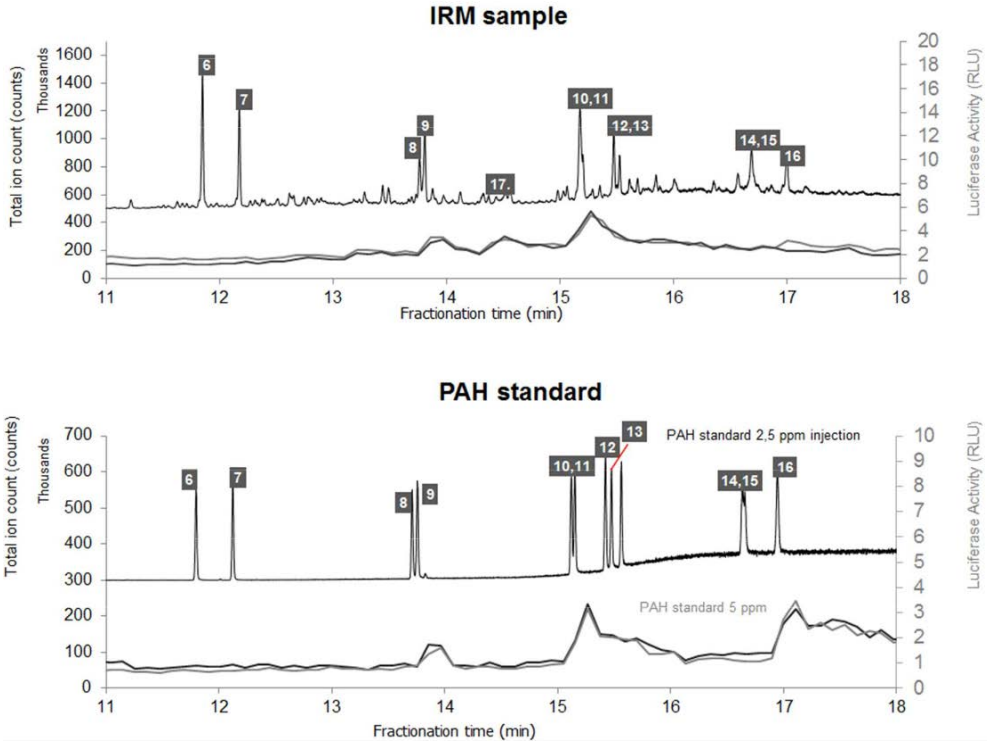

Figure S6. Expanded view of the bioactive area between 11 and 18 minutes displayed in Figure 4B and Figure 4C. Data has been plotted in an identical way where the MS data is superimposed on the bioassay data.

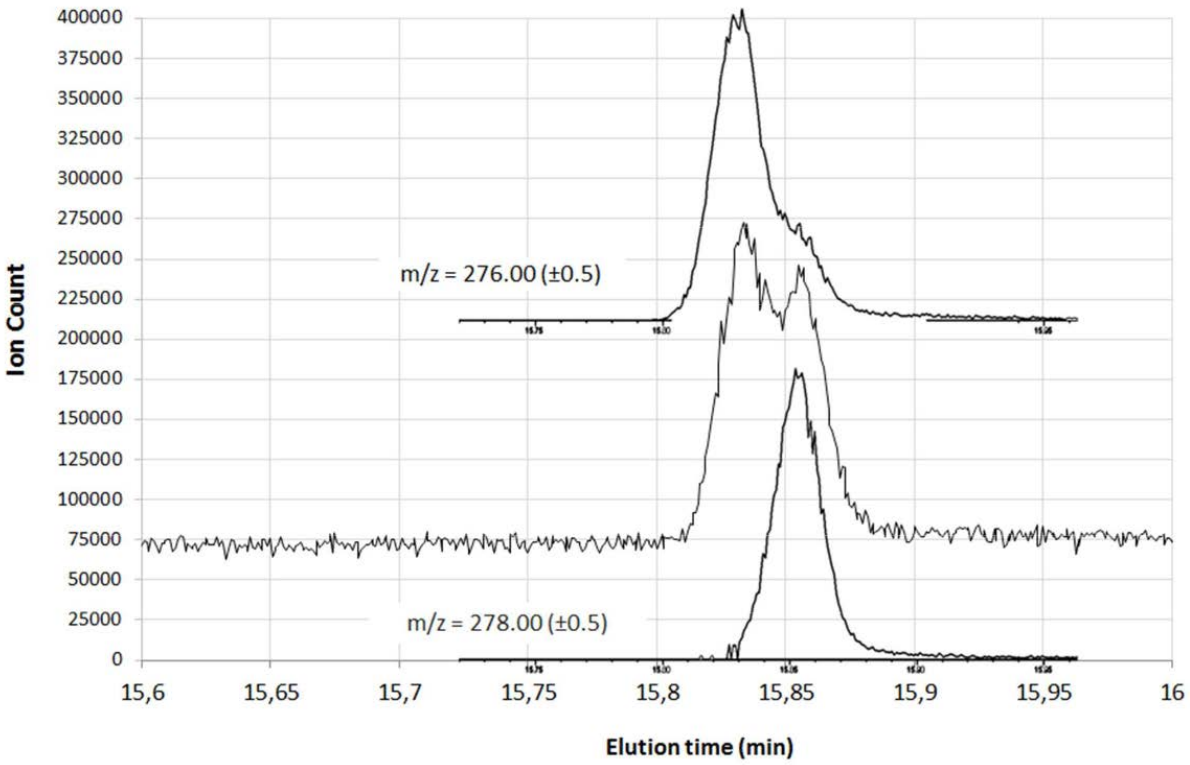

Figure S7A. A zoomed-in view of peak 15 in the chromatographic run of the PAH standard mixture. The extracted ion chromatograms (EIC) of *m/z* 276 (+/- 0.5) and *m/z* 278 (+/- 0.5) are shown together with the total ion chromatogram (TIC). Analysis of the MS fragmentation data from electron impact fragmentation using database comparison show that m/z 276 is caused by fragmentation of Indeno[1,2,3Acd]pyrene, while fragmentation of Dibenz[a,h]anthracene leads to an ion with *m/z* 278.

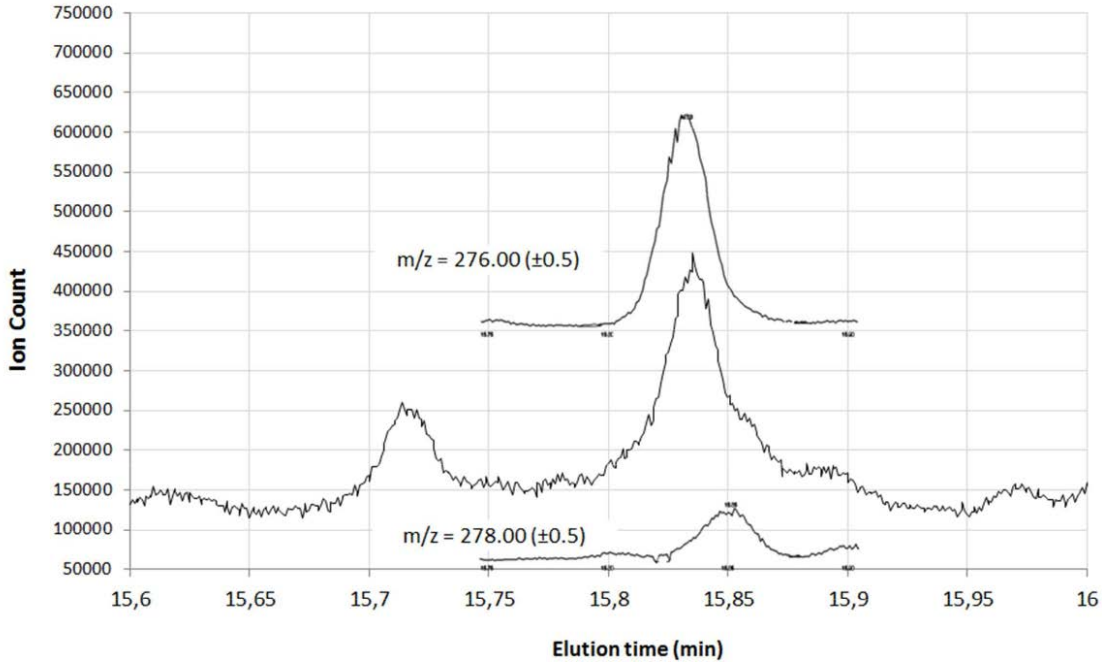

Figure S7B. A zoomed-in view of peak 15 in the chromatographic run of the CRM sample. The extracted ion chromatograms (EIC) of *m/z* 276 (+/- 0.5) and m/z278 (+/- 0.5) are shown overlaid with the total ion chromatogram (TIC). It can be seen that m/z 278 is barely present in the CRM sample, while m/z 276 is higher in abundance. Analysis of the ion peaks show that *m/z* 276 is caused by fragmentation of indeno[1,2,3Acd]pyrene, while fragmentation of dibenz[a,h]anthracene leads to *m/z* 278.

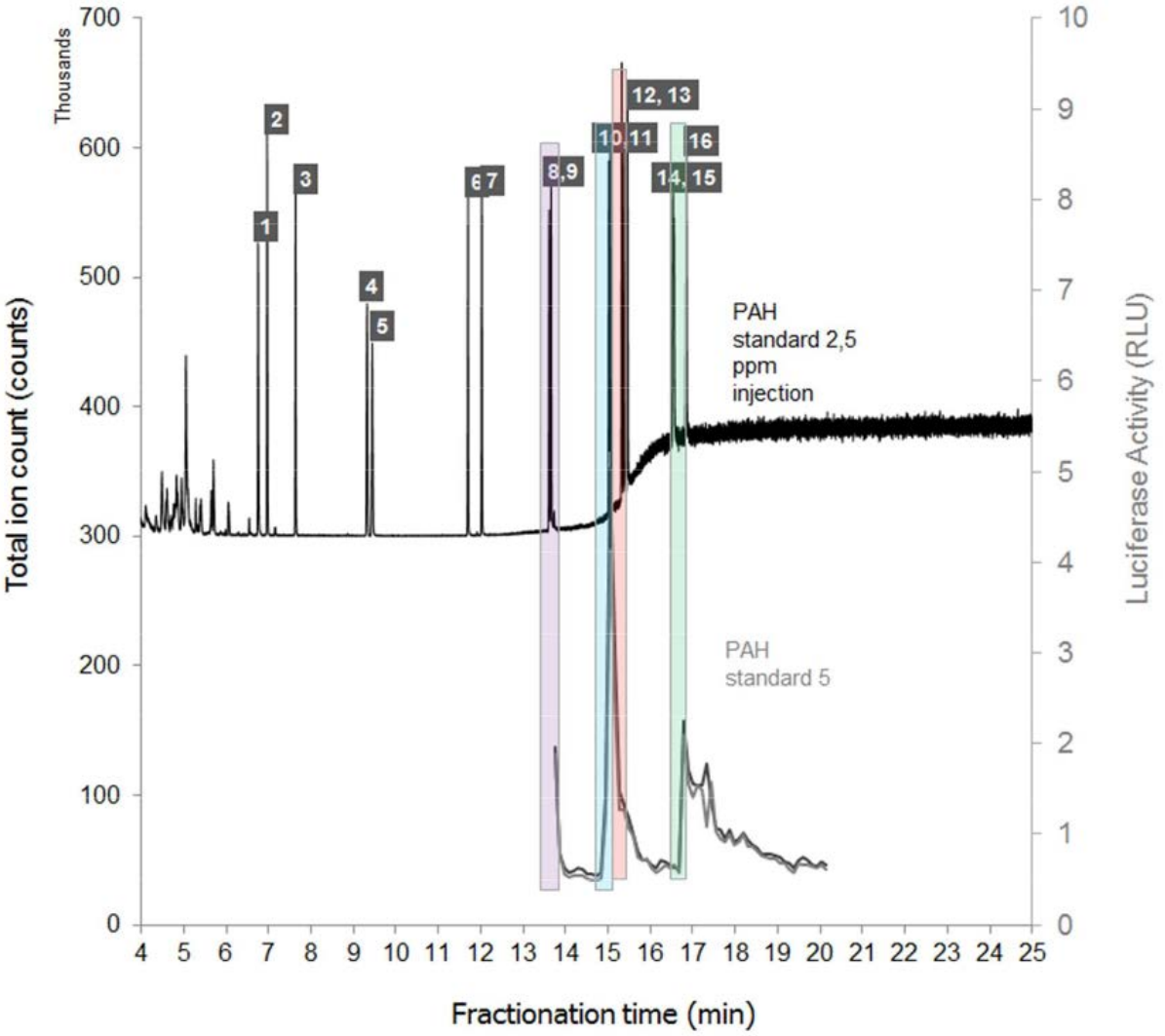

Figure S8A. Results of the experiment shown in Figure 5B repeated to evaluate the reproducibility of the analysis of the PAH sample. The results were very reproducible.

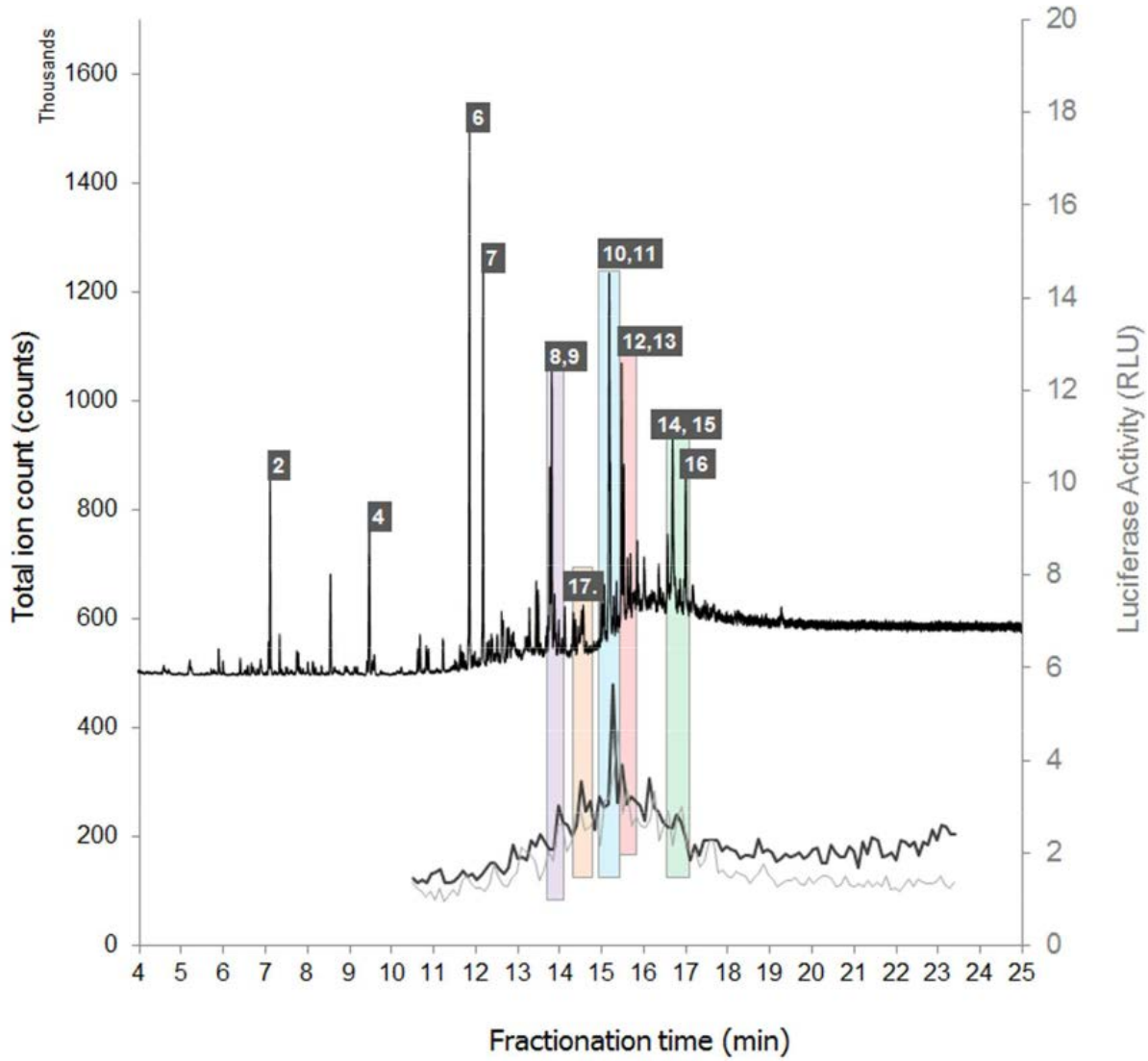

Figure S8B. Results of the experiment shown in Figure 5C repeated to evaluate the reproducibility of the analysis of the CRM sample. The results were very reproducible.

Table S1.
Recoveries and standard deviations of the fractions collected as shown in Figure S2B.

↓ flow (µL/min)	FCP	CPP	B	CFVP-b	4,4'-DBB
84	116% ± 3% 8% ± 1%	34% ± 7% 69% ± 18%	54% ± 21% 52% ± 17%	120% ± 44%	76% ± 10% 38% ± 2% 3% ± 2%
170	67% ± 35% 30% ± 29%	118% ± 3%	8% ± 11% 103% ± 13%	68% ± 96%	36% ± 15% 49% ± 21% 1% ± 0%
340	85% ± 7%	90% ± 1%	85% ± 5% 2% ± 0%	108% ± 7%	85% ± 8% 7% ± 10%